Polymer Chemistry

Accepted Manuscript

This is an *Accepted Manuscript*, which has been through the Royal Society of Chemistry peer review process and has been accepted for publication.

Accepted Manuscripts are published online shortly after acceptance, before technical editing, formatting and proof reading. Using this free service, authors can make their results available to the community, in citable form, before we publish the edited article. We will replace this *Accepted Manuscript* with the edited and formatted *Advance Article* as soon as it is available.

You can find more information about *Accepted Manuscripts* in the Information for Authors.

Please note that technical editing may introduce minor changes to the text and/or graphics, which may alter content. The journal's standard Terms & Conditions and the Ethical guidelines still apply. In no event shall the Royal Society of Chemistry be held responsible for any errors or omissions in this *Accepted Manuscript* or any consequences arising from the use of any information it contains.

ROYAL SOCIETY OF CHEMISTRY

www.rsc.org/polymers

Cite this: DOI: 10.1039/c0xx00000x

www.rsc.org/xxxxxx

PAPER

Poly(Vinyl Benzoate)-Backbone Mesogen-Jacketed Liquid Crystalline Polymers

Hong Yang,*[a] You-Jing Lv,[a] Ming Xu,[a] Jun Wang,[b] Bao-Ping Lin,[a] Ling-Xiang Guo,[a] and Er-Qiang Chen*[b]

Received (in XXX, XXX) Xth XXXXXXXXX 20XX, Accepted Xth XXXXXXXXX 20XX
DOI: 10.1039/b000000x

Previously reported polymer backbone structures of mesogen-jacketed liquid crystalline polymers (MJLCPs) to date are limited to polyacrylate, polystyrene, polyacetylene, polysiloxane, polythiophene and polynorbornene. In this manuscript, we describe a new system of MJLCPs with poly(vinyl benzoate)-backbone (**PVBnB**), which were synthesized by solution polymerization and bulk photo-polymerization method as well. Due to the low reactivity of vinylbenzoate group, we cannot achieve a high degree of polymerization. Ironically, benefiting from this low reactivity, we successfully prepared several loosely cross-linked MJLCP (**xPVBnB**) films with homogeneous- or homeotropic-alignment, for the first time by using UV-illumination on a unidirectional oriented mixture of vinylbenzoate monomers, crosslinkers and photo-initiators to perform polymerization and cross-linking at the same time, which are however extremely difficult for the much more reactive acrylate-type or styrene-type MJLCPs' precursor monomers due to the spontaneous thermal-polymerization reactions occurring at high temperatures. Experimental results show that **PVBnB** can form nematic or smectic phases depending on the alkyl chain length, **xPVBnB** films present very small elastomeric transformations (i.e. shrinkage/wrinkle) during the LC-to-isotropic phase transition.

1. Introduction

Mesogen-jacketed liquid crystalline polymers (MJLCPs),[1] as one special type of side-on side-chain liquid crystalline polymers (side-on SCLCPs)[2-15] with the waist or gravity center position of mesogenic unit linked to polymer backbone through a very short spacer or single carbon-carbon bond, have attracted tremendous scientific attention ever since the first discovery by Zhou et al. two decades ago.[16,17] MJLCPs present many fascinating properties, such as broad liquid crystalline (LC) temperature ranges, high glass transition temperatures, re-entrant isotropic phase, banded texture, and so on, mainly due to their unique molecular structures that rigid mesogenic units are closely packed around the polymer backbone, and the consequential strong steric hindrance forces the backbone to be well extended.[1]

Although there have been a lot of research works studying the relationships between the MJLCPs' mesomorphic properties and the varieties of laterally attached mesogenic cores, such as hydroquinone diester,[11,12] biphenyl,[18] terephthalate,[19] silsesquioxane,[20] bistolane,[21] thiophene,[22] oxadiazole,[23] and bent-cores,[24] as well as the lengths[25,26] and varieties[27] of peripheral chains, the previously reported polymer backbone systems of MJLCPs were very limited. Polyacrylate[11] (Fig. 1, Structure **1**) and polystyrene[12] (Fig. 1, Structure **2**) were the very first two examples and became the most popular backbone systems of MJLCPs thereafter. Chen et al. prepared polyacetylene (Fig. 1, Structure **3**) backbone MJLCPs *via* rhodium complex catalyzed polymerization in 2006.[28] Shen and Fan synthesized series of MJLCPs based on highly flexible polysiloxane main chain[29] (Fig. 1, Structure **4**), which could also assemble into supramolecular columnar nematic or smectic liquid crystalline phases compared to structurally similar MJLCPs having polyacrylate or polystyrene backbones. Zhou's group also invented polythiophene type MJLCPs (Fig. 1, Structure **5**) and the corresponding conjugated copolymers, meanwhile fabricated the polymeric light-emitting diode devices which showed excellent electroluminescence properties.[30] Pugh and Schrock described the first example of MJLCPs with two different polynorbornene backbones.[31-34] Our group reported in 2013 a series of MJLCPs and the corresponding mesogen-jacketed liquid crystalline elastomers (MJLCEs) containing a new polynorbornene backbone structure (Fig. 1, Structure **6**),[35] onto which the mesogens were laterally attached by a covalent carbon-carbon single bond without spacers. Very recently, Zhu et al. investigated the phase behaviors of a new series of MJLCP bearing a poly(norbornene-*exo*-dicarboximide) backbone, which presented amorphous and smectic A phases depending on the alkyl-tail length.[36]

Herein, we design and synthesize several novel MJLCPs, **PVBnB** (n represents the carbon number of the attached alkyl chain), possessing a new poly(vinyl benzoate) backbone (Fig. 1, Structure **7**). Mainly on the basis of wide-angle X-ray diffraction (WAXD) and polarized optical microscopy (POM), we

demonstrate that the **PVB4B** studied herein can exhibit a nematic phase with smectic C fluctuations, while **PVB10B** bearing a longer alkyl tail possesses an interdigitated smectic A phase.

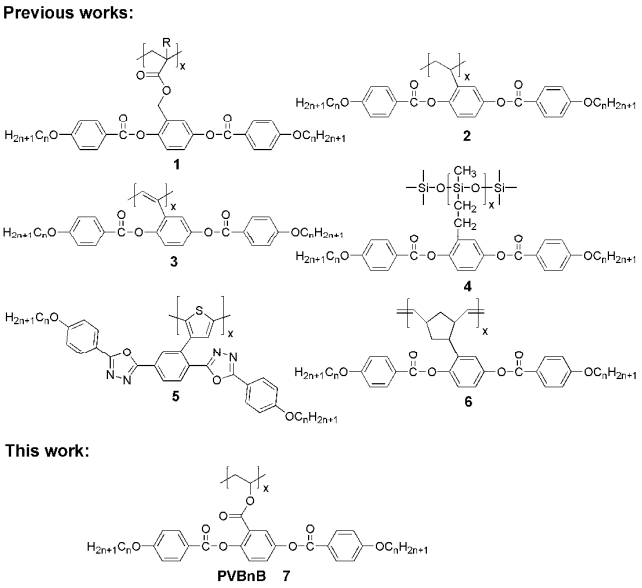

Fig. 1 The representative MJLCPs' backbone systems reported previously and herein this manuscript.

Traditional loosely cross-linked side-on SCLCPs with reasonably long spacers usually possess nematic or smectic phases, and the laterally-attached mesogens are always aligned along the polymer backbones' orientation so that the order-disorder transitions of mesogens can dramatically affect the backbones' order to achieve actuation functions.[37-39] However, as to MJLCPs, due to their unique mesogenic jacket structures, the mesogenic directors of side-chain are usually not parallel to the polymer backbones' orientations. This raises an interesting question of how the molecular arrangements and thermo-actuation properties of loosely cross-linked MJLCPs (xMJLCPs) behave. Recently, our group developed a method to prepare smectic mesogen-jacketed liquid crystalline elastomer (MJLCE) fibers by cross-linking pre-formed MJLCPs using a bifunctional benzophenone cross-linker[35] (Fig. S1A). However, the cross-linking sites are mainly located on the laterally-attached mesogen alkyl chains, while the polymer backbones are untouched. Herein, by UV-illumination on an oriented mixture of vinylbenzoate monomers and crosslinkers to perform polymerization and cross-linking at the same time, several xMJLCP (**xPVBnB**) films homogeneous- or homeotropic-aligned are successfully prepared. Most importantly, we can locate the cross-linking sites exactly on the polymer backbones (Fig. S1B) and study the effects of cross-linking sites influencing on the thermo-actuation properties of **xPVBnB** material.

2. Experimental Section

2.1. General Considerations

The starting materials and instrumentation descriptions, the detailed synthetic protocols and NMR spectra of compounds **9**, **11a**, **11b**, **12a**,[40] **12b**, **13a**, **13b**, **14**, **17, 18** are listed in the supporting information.

2.2. Synthesis of polymer PVBnB (7)

Typical procedure to prepare **PVB4B** *via* solution polymerization: **VB4B** (500 mg, 0.93 mmol), dicumyl peroxide (DCP, 25 mg, 0.09 mmol, 0.1 equiv) and dry DMF (0.5 mL) were added into a 25 mL Schlenk-type flask. The flask was degassed and exchanged with nitrogen *via* three freeze-thaw cycles. The reaction mixture was heated at 130 °C for 12 h and then poured into methanol (50 mL) to precipitate the polymer. The resulting polymer was further purified by dissolving in THF, reprecipitating from methanol several times, and dried in high vacuum, which gave the desired polymer **PVB4B** (356 mg, Yield: 71.2%) as a white solid.

Typical procedure to prepare **PVB4B** *via* bulk photo-polymerization: A solution of **VB4B** (200 mg, 0.37 mmol) and 2,2-dimethoxy-2-phenylacetophenone (photo-initiator, 1.0 mg, 0.004 mmol) in dry CH_2Cl_2 (0.3 mL) was casted into a 1.0 cm (length)×1.0 cm (width)×0.5 cm (depth) polytetrafluoroethylene (PTFE) tablet. After the solvent evaporated, the sample was placed in a zip-lock bag[41] with a stream of nitrogen, heated to 130 °C and then UV-illuminated for 2 h. THF (3 mL) was then used to fully dissolve the sample. The solution was poured into methanol (50 mL) to precipitate the polymer. The resulting polymer was further purified by dissolving in THF, reprecipitating from methanol several times, and dried in high vacuum, which gave the desired polymer **PVB4B** (130 mg, Yield: 65.0%) as a white solid.

2.3. Preparation of homogeneous-aligned xPVBnB film

Typical procedure to prepare **xPVB4B** film: **VB4B** (200 mg, 0.38 mmol), cross-linker **18** (9.2 mg, 0.02 mmol) and 2,2-dimethoxy-2-phenylacetophenone (photo-initiator, 1.0 mg, 0.004 mmol) were added into a 5 mL vial. The mixture was fully dissolved in 1 mL dry CH_2Cl_2, the solvent was then removed in *vacuo*. Mixtures, after heated in their isotropic phase (150 °C), were filled by capillarity in rubbed polyimide-coated glass cells of 20 micrometers gap (commercial Instec LC cells). The filled cells were slowly cooled down at -1 °C/min to the nematic phase (100 °C) of the mixture to achieve homogeneous alignment. After UV irradiation (365 nm, 20 mW/cm^2) under air atmosphere for 0.5 h, the free-standing, aligned **xPVB4B** films were obtained by dissolving the glass windows of the cells with 40% aqueous hydrofluoric acid solution.[42]

2.4. Preparation of homeotropic-aligned xPVBnB film

Following the above protocol, the mixtures were first filled into a surface-rubbed Instec LC cell to achieve homogeneous alignment at the nematic phase. An AC electric power (Variac, 50 Hz) was applied on the ITO regions of the LC cell (100 V, 5.0 V/μm) to homeotropically align the mesogens. After UV irradiation (365 nm, 20 mW/cm^2) for 0.5 h, the free-standing, aligned **xPVB4B** films were obtained by dissolving the glass windows of the cells with 40% aqueous hydrofluoric acid solution.

3. Results and Discussion

3.1. Synthesis

The synthetic procedures of the monomer **VBnB**, polymer **PVBnB** (n = 4 or 10) and the divinylbenzoate cross-linker are shown in Scheme 1. The carboxylic acid group of 2,5-dihydroxybenzoic acid **8** was first transformed to a benzyl ester, leaving two free hydroxyl groups which were then coupled with 4-alkyloxybenzoic acid **10** *via* DCC/DMAP protocol.[43] After benzyl-deprotection using Pd/C-catalyzed hydrogenation reaction, the key intermediates **12a** and **12b** were prepared following literature report.[40] Next step is an ester exchange reaction between vinyl acetate and intermediates **12**. After several experimental trials, we optimized this reaction by using $PdCl_2/CuBr_2$ catalyst system,[44] and successfully synthesized the vinylbenzoate monomers **VB4B** (**13a**) and **VB10B** (**13b**). Meanwhile, we also prepared an allylbenzoate monomer **AB4B** (**14**) by esterification of intermediate **12a** with allylbromide using TBAF as the base. Starting from 4-hydroxy-benzoic acid methyl ester **16**, the divinylbenzoate crosslinker **18** were synthesized through a three-step reaction route including Mitsunobu etherification,[45] saponification and ester exchanging.

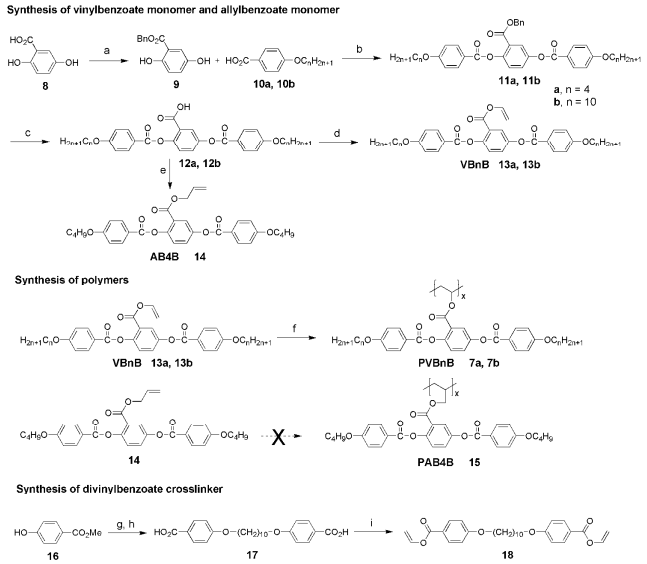

Scheme 1 Syntheses of monomers, polymers and divinylbenzoate crosslinker. Reagent and conditions: (a) BnBr, $NaHCO_3$, DMF, 70 ℃, 7 h; (b) DCC, DMAP, DCM, r.t., 12 h; (c) Pd/C, H_2, r.t., 12 h; (d) $PdCl_2$, $CuBr_2$, LiOAc, vinyl acetate, 70 ℃, 24 h; (e) allylbromide, TBAF, r.t., 2 h; (f) see Table 1; (g) decane-1,10-diol, DEAD, PPh_3, THF, r.t., 12 h; (h) LiOH, MeOH/ H_2O, reflux, 12 h; (i) $PdCl_2$, $CuBr_2$, LiOAc, vinyl acetate, 70 ℃, 24 h.

Table 1 Reaction conditions and results of radical polymerization of **VBnB**.

Entry	Polymer	Polymerization conditions	Polymer yield (%)	M_n (× 10^4 g/mol) [a]	PDI	T_d (℃) [b]
1	**PVB4B**	AIBN, toluene, 60 °C, 24 h	0	--	--	--
2	**PVB4B**	AIBN, toluene, 70 °C, 24 h	0	--	--	--
3	**PVB4B**	AIBN, toluene, 80 °C, 24 h	0	--	--	--
4	**PVB4B**	AIBN, DMF, 80 °C, 24 h	0	--	--	--
5	**PVB4B**	AIBN, DMF, 120 °C, 24 h	trace	--	--	--
6	**PVB4B**	AIBN, DMF, 140 °C, 24 h	trace	--	--	--
7	**PVB4B**	DCP, DMF, 130 °C, 24 h	71	1.15	1.56	284
8	**PVB4B**	UV irradiation, 130 °C, 2 h	79	2.97	1.49	285
9	**PVB10B**	UV irradiation, 130 °C, 2 h	88	5.71	1.35	286

[a]Molecular weight measurements were analyzed by GPC based on calibration using polystyrene standards. [b]The temperature at which 5% weight loss of the sample from TGA-DSC under nitrogen atmosphere at a heating rate of 10 °C/min.

Compared with acrylates, vinyl benzoate and allyl benzoate with a reverse rearrangement of the ester linking groups are much less reactive systems. To prepare the desired poly(vinyl benzoate) MJLCPs **PVBnB**, a tedious exploration of reaction conditions was performed. At first, we applied traditional radical polymerization methods using AIBN as the radical initiator, however, all the experimental trial results were negative (Table 1, Entry 1-4). Then, we realized that the reaction temperature might be a determining factor, and raised it to 120 ~ 140 °C (Table 1, Entry 5-6). Both trials provided trace amounts of polymer precipitates when dispersing in methanol. To improve the reaction yield, instead of AIBN whose 10 h half-life temperature is 65 °C in toluene, a high-temperature thermal-initiator, dicumyl peroxide (DCP) with a 10 h half-life temperature around 115 °C in benzene,[46] was used and successfully initiated the free radical polymerization (Table 1, Entry 7).

Besides the polymer synthesis in solution, we also applied UV light to photo-polymerize **VB4B** in neat conditions (bulk photo-polymerization). As described in the experimental section, **VB4B** was first casted as a thin film, which was then heated to above the melting point and exposed under UV illumination (20 mW·cm^{-2}, λ = 365 nm). The photo-reaction was monitored by FT-IR. As shown in Fig. 2, the absorption peak around 1750 cm^{-1} is attributed to the stretching vibration of C=C bond of the vinyl group. With the illumination time lengthening, a distinct reduction in the strength of the band at 1750 cm^{-1} is observed, which indicates that **PVB4B** can be efficiently prepared *via* photo-polymerization (Table 1, Entry 8). Following this UV illumination protocol, **PVB10B** can be also well-synthesized (Table 1, Entry 9). As to allylbenzoate monomer **AB4B** (**14**), neither solution polymerization nor bulk photo-polymerization methods did provide the designed poly(allyl benzoate)-backbone MJLCP **PAB4B** (**15**) due to the extremely low reactivity of allylbenzoate group as well as the high crystallizability of **AB4B**.

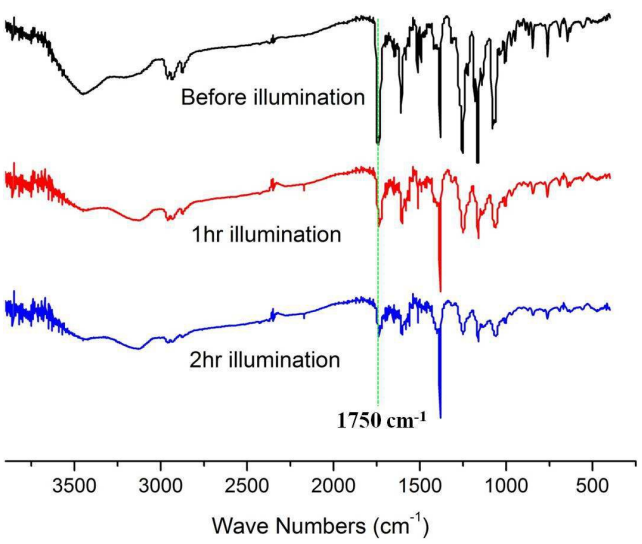

Fig. 2 FT-IR spectra of bulk photo-polymerization reaction of **VB4B** under UV irradiation for 0, 1 and 2 h, respectively.

^{1}H NMR spectra and the corresponding peak assignments of vinylbenzoate monomer **VB4B**, and the two polymers of **PVB4B** prepared by solution radical polymerization and bulk photo-polymerization, respectively, are shown in Fig. 3. The resonance signals of the side-on vinyl group, peak c at ~4.7 ppm and peak b at ~4.5 ppm can be ascribed to the two terminal olefin protons of the vinyl group, while the other olefin proton neighboring to the oxygen atom locates far downfield to ~7.5 ppm. The obvious disappearances of these three signals in polymers **PVB4B** present solid evidences for the two successful polymerizations. As observed by GPC showed in Table 1, bulk photo-polymerization technique in comparison with solution polymerization, can provide much higher molecular weight. The degradation temperatures at 5% weight loss (T_d's) of the three samples were determined by TGA under N_2, which are above 280 °C (Fig. S18), indicating that **PVBnB** have good thermal stabilities.

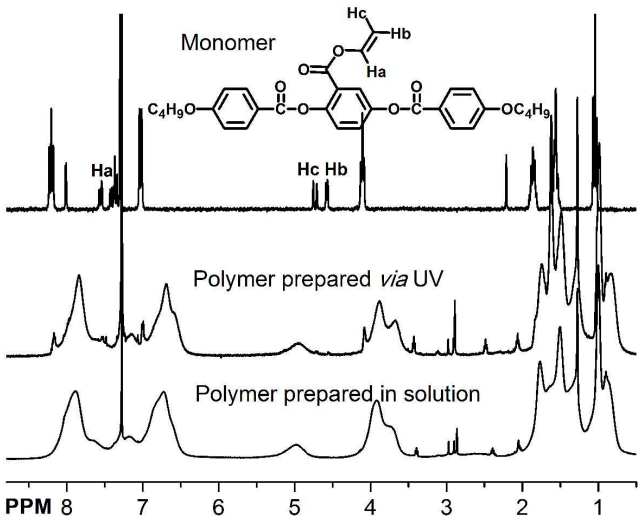

Fig. 3 ^{1}H NMR spectra of vinylbenzoate monomer **VB4B**, and the corresponding polymers **PVB4B** prepared by bulk photopolymerization and solution polymerization respectively.

3.2. Mesomorphic Properties of PVBnB

The thermal properties and mesomorphic behaviors of the novel poly(vinyl benzoate)-backbone MJLCPs synthesized were first investigated by DSC (Fig. 4) and POM (Fig. 5). The vinylbenzoate monomers **VB4B** and **VB10B**, both show two obvious reversible phase transition processes which are the crystal melting and the isotropization, respectively. Based on the observed marble textures shown in Fig. 5A-B and the thread-like texture recorded in Fig. 5E, **VB4B**, **VB10B** and **AB4B** possess one single enantiotropic nematic phase, the detailed transition temperatures are described in the supporting information.

PVB4B prepared by solution polymerization presents one enantiotropic LC phase with a typical schlieren-like texture (Fig. 5C) between the glassy and the isotropic state (Fig. S19). Interestingly, the LC-isotropic phase transition temperature of **PVB4B** is lower than the clearing point of the precursor monomer **VB4B**. However, **PVB4B** prepared by bulk photo-polymerization possesses only the glass transition (Fig. 4B) and shows very weak birefringence (Fig. 5D) along with the temperature being raised up to decomposition point. The key difference between these two **PVB4B** polymers obtained by different methods is the molecular weight. Solution polymerization provides short oligomers which might behave more like small molecules having characteristic texture and lower phase transition temperature. On the contrary, the mesomorphic properties of high molecular weight **PVB4B** polymer prepared by bulk photo-polymerization are markedly influenced by high viscosity and intrinsic "mesogen-jacket" effect.[1] Hereinafter, we will focus on **PVBnB** prepared by bulk photo-polymerization.

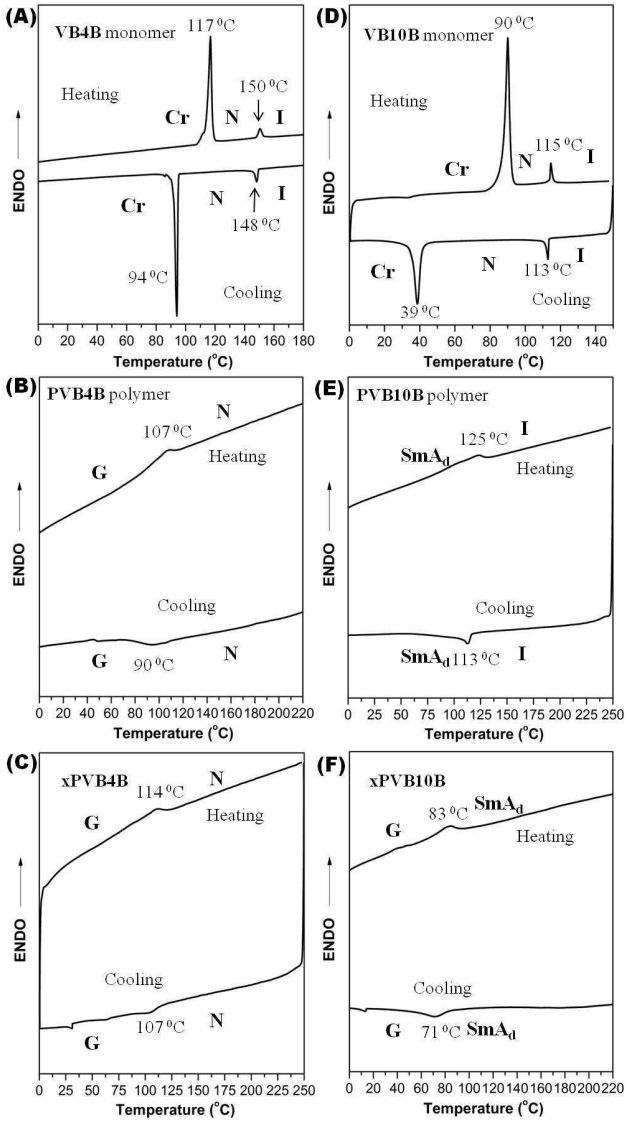

Fig. 4 DSC curves of (A) monomer **VB4B**, (B) polymer **PVB4B** prepared by bulk photo-polymerization, (C) the corresponding crosslinked MJLCP **xPVB4B**, (D) monomer **VB10B**, (E) polymer **PVB10B** prepared by bulk photo-polymerization, (F) the corresponding crosslinked MJLCP **xPVB10B** on first cooling and second heating cycle. Cr = crystalline, N = nematic, SmA_d = interdigitated smectic A, I = isotropic, G = glass phase.

1D WAXD experiments were performed to elucidate the mesomorphic phase of **PVB4B** and **PVB10B** prepared by bulk photo-polymerization. As presented in Fig. 6A-B, the WAXD profiles of **PVB4B** powder sample show two diffuse peaks in low- and wide-angle region, respectively. The diffuse peak at low angles (2θ = 4.15°) with a *d*-spacing of ~2.13 nm should be associated with the length of the laterally-attached mesogen of 1,4-di(4'-butyloxybenzoyloxy)benzene. However, compared with the fully extended mesogen length (l = 2.75 nm) estimated by Dreiding models, the observed *d* spacing is relatively shorter. It is observed that the low-angle peak intensity of **PVB4B** is larger at higher temperatures, which is one characteristic of MJLCPs' scattering.[47] On the contrary, the 1D WAXD profiles (Fig. 6C-D) of **PVB10B** powder sample show one sharp and intense diffraction peak in low-angle region (2θ = 2.68°) with a *d*-spacing of ~3.30 nm, indicating clearly the existence of LC structure.

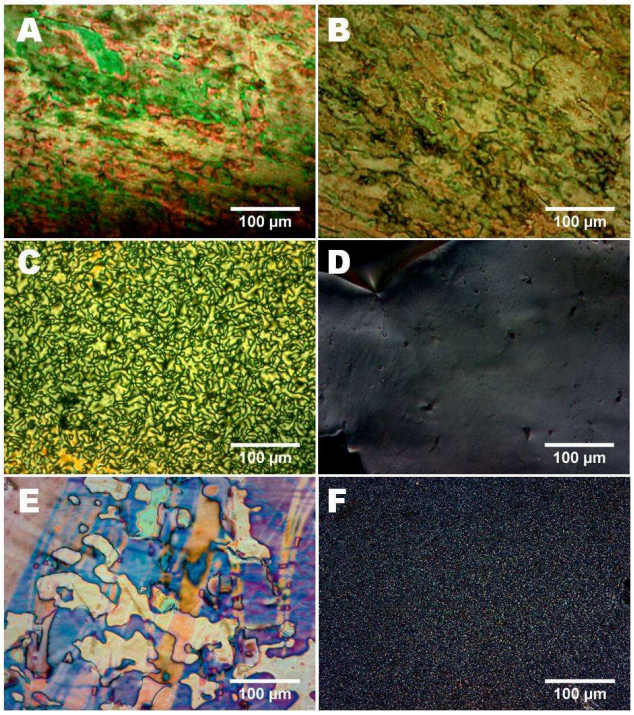

Fig. 5 Polarized optical microscope images of (A) **VB4B** maintained at 120 °C, (B) **AB4B** maintained at 90 °C, (C) **PVB4B** prepared by solution polymerization, maintained at 90 °C, (D) **PVB4B** prepared by bulk photo-polymerization, maintained at 130 °C, (E) **VB10B** maintained at 100 °C, and (F) **PVB10B** prepared by bulk photo-polymerization, maintained at 100 °C.

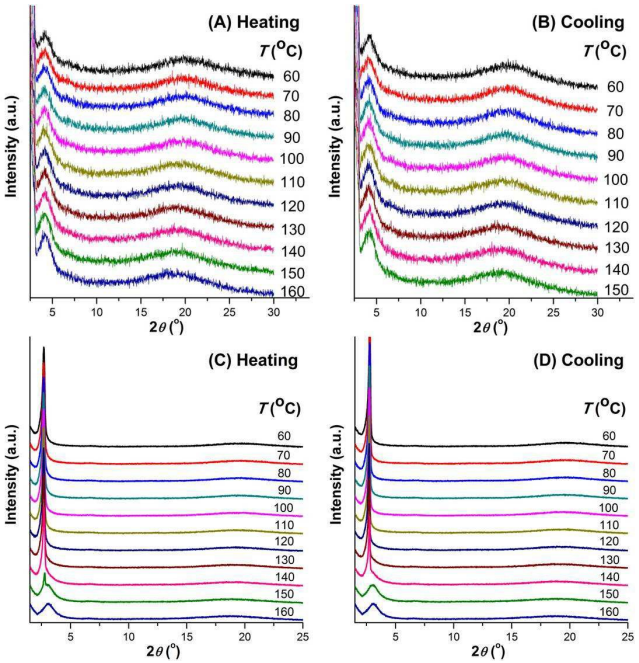

Fig. 6 One-dimensional WAXD profiles of **PVB4B** on (A) heating and (B) cooling, and **PVB10B** on (C) heating and (D) cooling.

2D WAXD experiments were further carried out on oriented **PVBnB** samples (Fig. 7A) which were mechanically sheared at 180 °C followed by annealing for several hours.[47-53] Fig. 7B-C illustrates the 2D WAXD pattern of a unidirectional oriented **PVB10B** sample recorded at room temperature with the X-ray incident beam either perpendicular (along Z axis, i.e. the shear

gradient shown in Fig. 7A) or parallel to the shear direction (X axis). As shown in Fig. 7B, when the shear direction is parallel to the equator direction, a pair of intense arcs in low-angle region is located on the meridian direction. On the other hand, when the X-ray beam is parallel to the shear direction, the pair of diffractions appears on the equator which is the Z axis (Fig. 7C). As only the first order diffraction is detected, the LC structure of **PVB10B** is hard to be determined unambiguously. Nevertheless, combining the 2D WAXD patterns recorded along two directions, we consider that, most likely, **PVB10B** forms a smectic structure. During mechanical shearing, the main-chains can be aligned along shear direction; however, the smectic layer may be either perpendicular or parallel to the shear plane (X-Y plane in Fig. 7A), which can give the diffraction pattern of Fig. 7B and 7C, respectively. Note that the layer thickness (~3.27 nm) is much shorter than the fully extended mesogen length (l = 4.25 nm) of the laterally-attached mesogen, 1,4-di(10'-decyloxybenzoyloxy)benzene estimated by Dreiding models. The mesomorphic phase of **PVB10B** can be interdigitated smectic A (SmA_d), as the typical quadruple scattering halo of Smectic C (SmC) phase was not observed in high-angle region (Fig. 7B-C).

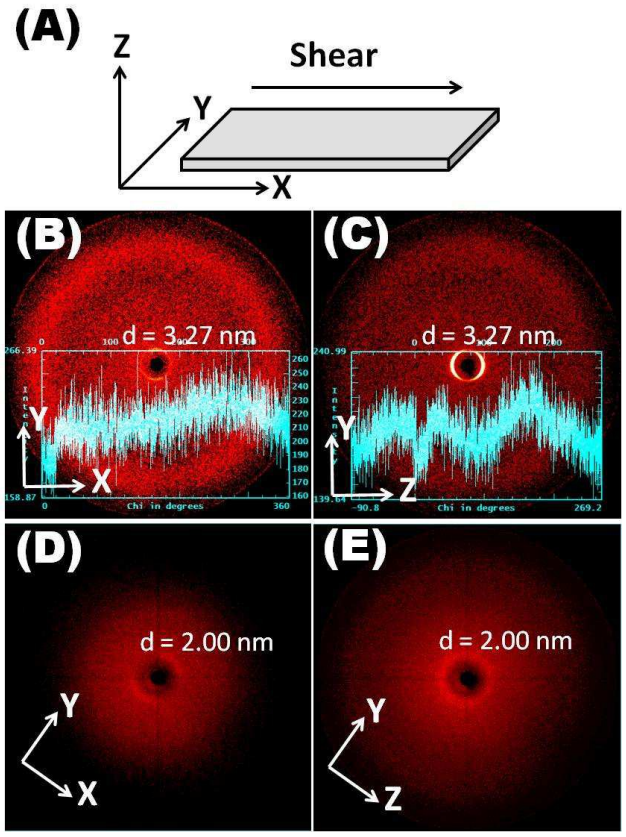

Fig. 7 (A) Schematics of shearing geometry. Two-dimensional WAXD pattern (azimuthal scan in the high-angle region) of sheared **PVB10B** sample recorded at room temperature with the X-ray incident beam along (B) Z direction and (C) X direction. Two-dimensional WAXD pattern of sheared **PVB4B** sample recorded at room temperature with the X-ray incident beam along (D) Z direction and (E) X direction.

As to **PVB4B** sample, when X-ray beam was incident perpendicular (along Z axis) to the shear direction (Fig. 7D), a pair of diffused arcs in low-angle region with *d*-spacing of ca. 2.0 nm is observed with the intensity more or less concentrated on the line perpendicular to the shear direction. Fig. 7E exhibits an isotropic intensity distribution when X-ray incident beam was parallel (along X axis) to the shear direction. The diffraction result shown in Fig. 7D-E looks quite similar to that observed from other MJLCPs with a supramolecular columnar nematic (Φ_N) phase.[47] This implies that the **PVB4B** chains may adopt a rod-like conformation as a whole with the lateral dimension of ~2.0 nm, packing together with a nematic fashion. However, considering the smectic structure of **PVB10B** analogue and the 2D WAXD profile of homogeneous-aligned **xPVB4B** film (see below), **PVB4B** sample is more likely to possess a nematic phase with smectic C fluctuations.[49] For the nematic with smectic C fluctuations, while the **PVB4B** main chains were preferentially aligned by mechanical shearing, the mesogenic side chains tilting ~50° away from the main chain axis may form a smectic C-like layer structure with the periodicity of ~2.0 nm on average.

3.3. Preparation and Mesomorphic Properties of Cross-Linked MJLCP Films

In recent years, loosely cross-linked LC polymers (also known as liquid crystalline elastomers, LCE) with their versatile shape-transformation abilities under external stimuli (thermal,[54] light,[55,56] electrical,[57] magnetic,[58] etc.) have been intensively investigated and applied as mechanical actuators,[59] smart surfaces,[41,60] artificial organs,[61] chemical sensors,[62] and miniaturized devices.[63-66] The key of synthesizing monodomain LCEs is to form a unidirectional aligned cross-linked network. Among several representative LCE preparation protocols,[39] using anti-parallel surface-rubbed LC cells to fabricate LCE films directly starting from small molecules is a very convenient and efficient method.[40,67] This protocol usually includes three steps: 1) fill the mixture of liquid crystalline monomers and crosslinkers into LC cells, after raising the temperature to the isotropic phase, 2) lower the temperature to the LC phase, perform polymerization and crosslinking at the same time; 3) open the LC cells to get LCE films. However, previously there was no any report of preparing oriented xMJLCP samples by using this approach, because the clearing points of traditional acrylate-type or styrene-type monomers of MJLCPs were very high and it was extremely difficult to fill these monomers into LC cells by capillarity, due to the spontaneous thermal-polymerization reactions occurring at high temperatures.

In our case, thanks to the low reactivity of vinylbenzoate group, **VBnB** monomers are quite thermal-stable above their clearing points and can survive at 150 °C for several hours without self-polymerization, which provide us an opportunity to prepare xMJLCP films for the first time. As described in the experimental section, we first developed a novel divinylbenzoate crosslinker **18** which might have similar reactivity with **VBnB** so that it could be well dispersed into the monomers and the corresponding xMJLCP network, thereafter a 20 μm thick homogeneous-aligned **xPVB4B** film was synthesized. Under POM observation, the homogeneous-alignment effect of this **xPVB4B** film is almost perfect. As indicated in Fig. 8A-C, the film shows excellent extinction when the film's surface-rubbing direction is parallel or perpendicular to the analyzer. Rotation of the film by 45° maximizes the transmission from extinction. Homogeneous-aligned **xPVB10B** films are also successfully prepared following

the above described protocol. As shown in Fig. S20, the lamellar structure's focal conic defect lines are more or less parallel to the surface rubbing direction, thus the uniformity of the alignment is qualitatively good.

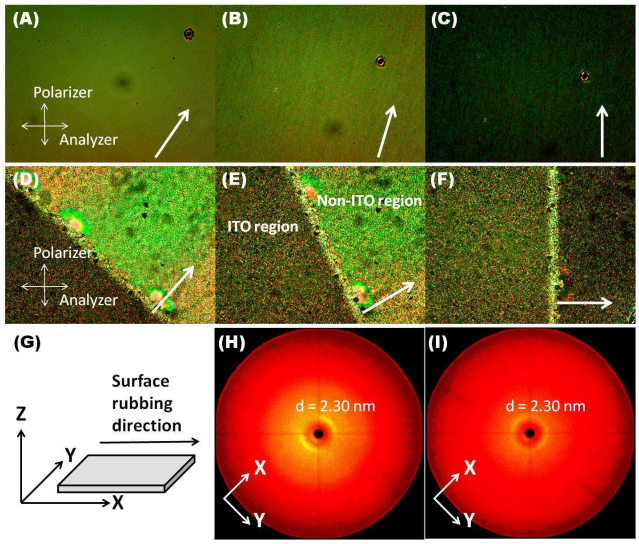

Fig. 8 (A-C) Polarized optical microscope images of a homogeneous-aligned **xPVB4B** film, the white arrow represents the surface-rubbing direction. (D-F) Polarized optical microscope images of a homeotropic-aligned **xPVB4B** film, the left region is ITO-coated area and the right region has no ITO. (G) Schematics of surface rubbing geometry. (H) 2D WAXD pattern of a homogeneous-aligned **xPVB4B** film recorded at room temperature with the X-ray incident beam parallel to the film normal direction. (I) 2D WAXD pattern of a homeotropic-aligned **xPVB4B** film recorded at room temperature with the X-ray incident beam parallel to the film normal direction.

We also prepared a 20 μm thick homeotropic-aligned **xPVB4B** film by applying an AC electric power on the ITO regions of the anti-parallel surface-rubbed LC cell (100 V, 5.0 V/μm) to vertically align the pre-filled mesogens and then performing UV-illumination. The ideal scenario of a perfect homeotropic alignment is to observe a full extinction of birefringence at any rotation angles under POM. As indicated in Fig. 8D-F, when rotating the **xPVB4B** film, the POM image of ITO-coated region always shows very low transmission while the transmission of the non-ITO-coated region changes dramatically depending on the rotation degree between the film's surface-rubbing direction and the analyzer director. These two obviously different phenomena indicate that the mesogens in non-ITO-coated area are homogeneous-aligned while the mesogens in ITO-coated area are homeotropic-aligned, although the presence of weak birefringence implies a modest alignment effect. This imperfectness might be due to the AC power source being provided in this experiment by a simple 50 Hz Variac, instead of a delicate set-up using high-frequency signal generator and high-voltage amplifier.

2D WAXD experiments were performed on the homogeneous- and homeotropic-aligned **xPVB4B** films. As shown in Fig. 8H, with the X-ray beam parallel to the normal direction of the homogeneous-aligned **xPVB4B** film, two low-angle diffraction arcs can be clearly observed. This indicates that mesogens have a good unidirectional in-plane order, and thus the **PVB4B** chains are lying down. As to the homeotropic-aligned **xPVB4B** film, the X-ray incident beam along the in-plane direction of the film could not give information due to the very thin film thickness. On the other hand, when the X-ray beam was also parallel to the normal direction of the homeotropic-aligned **xPVB4B** film, a low intensity diffraction ring locates in the low-angle region (Fig. 8I), indicating that the homeotropic alignment effect is modest.

The POM and WAXD results of homogeneous-aligned **xPVB4B** support that a nematic phase with smectic C fluctuations instead of Φ_N exists in **PVB4B** system. Fig. 8H renders the 2D WAXD same as that shown in Fig. 7D of the sheared **PVB4B**, suggesting the two samples sharing a same structure. Combining the POM observation, we conclude that mesogens in the **xPVB4B** film are all lying down in the film plane. This orientation in fact is unfavorable to the formation of columnar phase which takes of rod-like MJLCP chains with the side chains wrapping around the backbone as the building block. In this case, we consider that the low-angle scattering with a relatively shorter *d*-spacing comparing with the full length of the laterally-attached mesogen (2.30 nm vs. 2.75 nm) is associated with the mesogens not only arranged in a nematic orientation but also tilted to the polymer main chains, which forms the nematic with smectic C fluctuations as illustrated in Fig. S1B.

The thermal properties and mesomorphic behaviors of **xPVB4B** film were investigated by DSC, and only one transition at ~114 °C is observed (Fig. 4C). To differentiate between the possibilities of glass phase transition, LC-LC phase transition or LC-isotropic phase transition, we performed POM experiments upon heating. As shown in Fig. 9, although the birefringence of **xPVB4B** film changes during the phase transition, a completely dark texture is not observed, which implies that the LC-isotropic phase transition is absence along with the temperature being raised up to 250 °C, which is close to the degradation (5% weight loss) temperature ~285 °C as shown in Fig. S18.

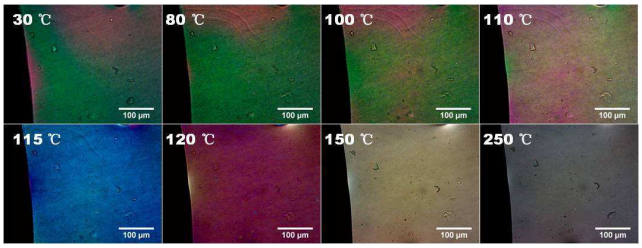

Fig. 9 Polarized optical microscope images of a homogeneous-aligned **xPVB4B** film stripe recorded at 30, 80, 100, 110, 115, 120, 150 and 250 °C during heating process.

Moreover, we applied thermal 2D WAXD technique to further study the **xPVB4B**'s molecular arrangement at various temperatures. As illustrated in Fig. S21, below the transition temperature detected by DSC (i.e., 90, 100, 110 °C), this **xPVB4B** film presents well-oriented low-angle sharp diffraction arcs, almost same to that recorded at room temperature (Fig. 8H). Furthermore, in the high-angle region, a pair of scattering halos with a broad azimuthal is observed, indicating a short-range sub-nanometer scale order. After the **xPVB4B** film has been heated to above the transition temperature (130 and 140 °C), careful examination reveals that the original low-angle diffraction arcs still retain on XRD patterns at nearly the same location, although the intensity becomes lower. This phenomenon indicates that in this transition process, the order parameter decreases while

molecular orientations and arrangements remain largely unchanged. Thus, the only transition of **xPVB4B** film observed by DSC is neither LC-isotropic phase transition nor a LC-LC phase transition, but the glass phase transition.

In the case of **xPVB10B** sample, only one transition in the temperature range of 71-83 °C is observed (Fig. 4F). Further POM investigation (Fig. S22) indicates that unlike **xPVB4B** sample having no clearing point, **xPVB10B** has an apparent LC-isotropic phase transition at ca. 130 °C, which is also verified by 2D WAXD experiments. As shown in Fig. S23, the low-angle diffraction would disappear at 140 °C, indicating an obvious order-to-disorder transition at 130~140 °C. This result suggests that lengthening the alkyl chains is an efficient strategy to make **xPVBnB** material prone to form better smectic structures and meanwhile possess the LC-isotropic phase transition.

3.4. Thermal-Actuation Effects of Cross-Linked MJLCP Films

The thermal-actuation effects of two homogeneous-aligned xMJLCP (**xPVB4B** and **xPVB10B**) films were also studied. In the experiment, a homogeneous-aligned xMJLCP film was placed on a microscope slide which had been surface-treated with several drops of silicone oil or sea sands to prevent film sticking onto the glass. The microscope slide was then placed on a hot stage and heated from 30 to 200~250 °C. As shown in Fig. 10A, along with the temperature variation, no shrinkage or elastomeric transformation of this homogeneous-aligned **xPVB4B** film can be observed, which further proves that this **xPVB4B** network has no isotropic phase till decomposition. In the case of **xPVB10B** film, only a slight wrinkle/shrinkage phenomenon with a maximum shape variation of less than 5% during the LC-isotropic transition was recorded at Fig. 10B and S1.avi.

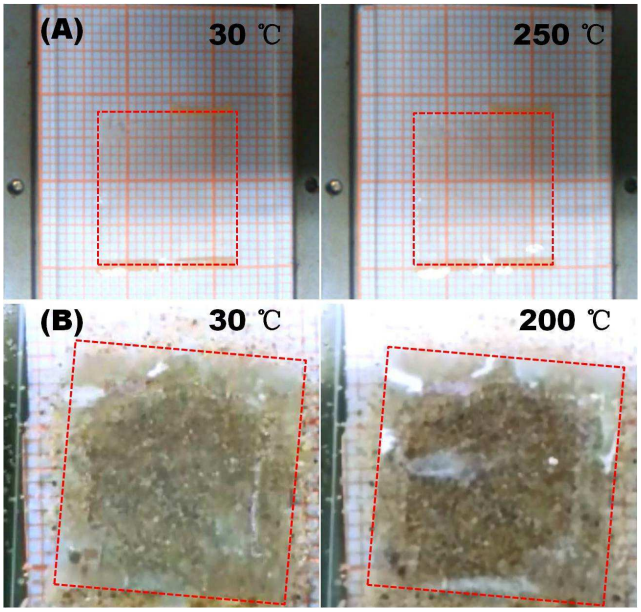

Fig. 10 Photographs of homogeneous-aligned (A) **xPVB4B** film heated at 30 ℃ and 250 ℃ respectively (The yellow stripe edges are the glued 20 μm thick spacers.), (B) **xPVB10B** film heated at 30 ℃ and 200 ℃ respectively. The dashed line rectangles which outline the shapes of **xPVBnB** films are drawn as a visual guide.

These xMJLCP films' inelasticity phenomena have never been observed in traditional side-on side-chain LCE systems. Our hypothesis is that the mesogenic directors, polymer main chain orientations and crosslinking sites markedly influence the thermal-actuation abilities of xMJLCP materials. As illustrated in Fig. 11A, laterally-attached mesogens of side-on side-chain LCEs are always aligned along the polymer backbones' orientations, thus beyond the clearing point, disorientation of mesogens will disturb and coil the main chains so that the crosslinked LCE network will shrink along the original alignment direction. As to xMJLCP systems, mesogenic directors are tilted to the polymer main chain orientations due to the mesogenic jacketing effect, which forces mesogens and polymer backbone to form two relatively independent architectures. If the cross-linking sites are located on the laterally-attached mesogen alkyl chains (Fig. 11B), the crosslinked mesogens form into a network which is similar to main-chain LCE system to some extent. The LC-isotropic transition disorders the mesogenic directors so that the xMJLCP backbones are drawn close to each other and the whole material shrinks along the original mesogenic orientation.[35] However, if the cross-linking sites are located on polymer main chains (Fig. 11C), the bonded backbones and crosslinkers will form a stable and fixed frame-like network, which are hung with mesogens. Since the mesogens are already tilted to the backbones, disordering of mesogenic directors makes little impact on the base frame-like network, which explains the small shrinkage effect of **xPVB10B** films.

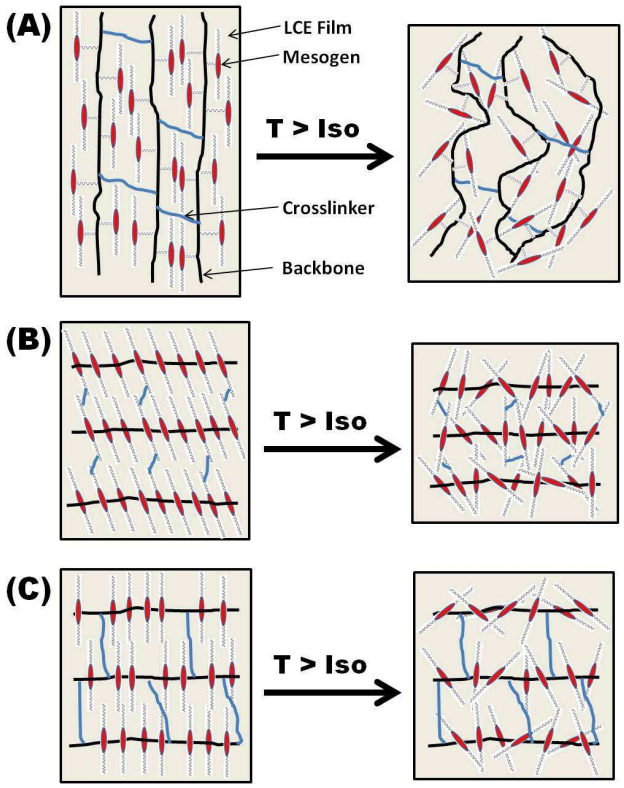

Fig. 11 Schematic explanation of the thermal-actuation effects of homogeneous-aligned (A) traditional side-on side-chain LCE films, (B) alkyl-tail-crosslinked MJLCE films and (C) backbone-crosslinked MJLCE films.

Conclusions

In conclusion, we design a new type of mesogen-jacketed liquid crystalline polymers **PVBnB** (n = 4, 10) bearing poly(vinyl benzoate) backbone and synthesize them successfully *via* solution polymerization and bulk photo-polymerization. Due to the low reactivity of vinylbenzoate group, we cannot achieve a high degree of polymerization. Solution polymerization provides short oligomers with a number-average M_n ~ 11 kDa, while bulk photo-polymerization is more efficient and prepares relatively higher molecular weight polymers with a M_n ~ 30-60 kDa. The mesomorphic properties of these polymers are markedly influenced by the molecular weight. On the basis of diffraction features, we propose that the **PVB4B** obtained by bulk photo-polymerization can form a nematic phase with smectic C fluctuations, which is rather stable in the whole temperature range up to the decomposition temperature, and the **PVB10B** analogue bearing much longer alkyl tails can form an interdigitated smectic A phase.

Taking advantage of the low reactivity of vinylbenzoate group and high thermal-stability of monomers, we successfully prepare several xMJLCP films with homogeneous- or homeotropic-alignment, for the first time, by UV-illumination on a unidirectional oriented mixture of vinylbenzoate monomers, crosslinkers and photo-initiators to perform polymerization and cross-linking at the same time. These loosely cross-linked MJLCP networks with only 5 mol% cross-linking density exhibit the well-aligned LC orders and present however very small elastomeric transformations (i.e. shrinkage/wrinkle) during even the LC-to-isotropic phase transition.

Further elucidation of mesomorphic behaviors of poly(vinyl benzoate)-backbone MJLCPs with alkyl tail length variations, as well as the molecular structures and mechanical properties of xMJLCPs derived from this basic strategy, are under investigation. This will be the subject of a future publication.

Acknowledgement

This research was supported in part by National Natural Science Foundation of China (Grant No. 21374016, 51273002, 21474002) and the Major State Basic Research Development Program (2011CB606004) from the Ministry of Science and Technology.

Notes and references

[a] *School of Chemistry and Chemical Engineering, Jiangsu Province Hi-Tech Key Laboratory for Bio-medical Research, Jiangsu Optoelectronic Functional Materials and Engineering Laboratory, Southeast University, Nanjing 211189, China. Fax: 86 25 52091096; Tel: 86 25 52091096; E-mail: yangh@seu.edu.cn.*

[b] *Beijing National Laboratory for Molecular Sciences, Key Laboratory of Polymer Chemistry and Physics at the Ministry of Education, College of Chemistry and Molecular Engineering, Peking University, Beijing 100871, China. Fax: 86 25 62753370; Tel: 86 25 62753370; E-mail: eqchen@pku.edu.cn.*

† Electronic Supplementary Information (ESI) available: See DOI: 10.1039/b000000x/

1 X. F. Chen, Z. H. Shen, X. H. Wan, X. H. Fan, E. Q. Chen, Y. G. Ma and Q. F. Zhou, *Chem. Soc. Rev.*, 2010, **39**, 3072-3101.

2 H. Finkelmann, H. Ringsdorf and J. H. Wendorff, *Makromol. Chem., Macromol. Chem. Phys.,* 1978, **179**, 273-276.

3 F. Hessel and H. Finkelmann, *Makromol. Chem., Macromol. Chem. Phys.,* 1988, **189**, 2275-2283.

4 V. Percec and R. Rodenhouse, *J. Polym. Sci., Part A: Polym. Chem.,* 1991, **29**, 15-28.

5 V. Percec, J. Heck and G. Ungar, *Macromolecules,* 1991, **24**, 4957-4962.

6 V. Percec and D. Tomazos, *J. Mater. Chem.,* 1993, **3**, 643-650.

7 V. Percec and D. Tomazos, *Adv. Mater.,* 1992, **4**, 548-561.

8 V. Percec, A. D. Asandei and P. Chu, *Macromolecules,* 1996, **29**, 3736-3750.

9 V. Percec, A. D. Asandei, D. H. Hill and D. Crawford, *Macromolecules,* 1999, **32**, 2597-2604.

10 M. F. Achard, N. Leroux and F. Hardouin, *Liq. Cryst.,* 1991, **10**, 507-517.

11 G. W. Gray, J. S. Hill and D. Lacey, *Mol. Cryst. Liq. Cryst.,* 1991, **197**, 43-55.

12 F. Hardouin, N. Leroux, S. Mery and L. J. Noirez, *Phys. II,* 1992, **2**, 271-278.

13 N. Leroux, P. Keller, M. F. Achard, L. Noirez and F. J. Hardouin, *Phys. II,* 1993, **3**, 1289-1296.

14 S. Lecommandoux, M. F. Achard, F. Hardouin, A. Brulet and J. P. Cotton, *Liq. Cryst.,* 1997, **22**, 549-555.

15 A. Cherodian, M. Hughes, L. Noirez and F. Hardouin, *Liq. Cryst.,* 1994, **16**, 421-428.

16 Q. F. Zhou, H. M. Li and X. D. Feng, *Macromolecules,* 1987, **20**, 233-234.

17 Q. F. Zhou, X. L. Zhu and Z. Q. Wen, *Macromolecules,* 1989, **22**, 491-493.

18 L. Zhang, H. Wu, Z. H. Shen, X. H. Fan and Q. F. Zhou, *J. Polym. Sci. Part A: Polym. Chem.,* 2011, **49**, 3207-3217.

19 H. L. Tu, D. Zhang, X. H. Wan, X. F. Chen, Y. X. Liu, H. L. Zhang and Q. F. Zhou, *Macromol. Rapid Commun.,* 1999, **20**, 549-551.

20 Q. W. Pan, L. C. Gao, X. F. Chen, X. H. Fan and Q. F. Zhou, *Macromolecules,* 2007, **40**, 4887-4894.

21 Z. L. Zhang, L. Y. Zhang, Z. H. Shen, G. Z. Xing, X. H. Fan and Q. F. Zhou, *J. Polym. Sci. Part A: Polym. Chem.,* 2010, **48**, 4627-4639.

22 Q.Yang, Y. Xu, H. Jin, Z. Shen, X. Chen, D. Zou, X. Fan and Q. Zhou, *J. Polym. Sci., Part A: Polym. Chem.,* 2010, **48**, 1502-1515.

23 C. P. Chai, X. Q. Zhu, P.Wang, M. Q. Ren, X. F. Chen, Y. D. Xu, X. H. Fan, C. Ye , E. Q. Chen and Q. F. Zhou, *Macromolecules,* 2007, **40**, 9361-9370.

24 X. F. Chen, K. K. Tenneti, C. Y. Li, Y. W. Bai, R. Zhou, X. H. Wan, X. H. Fan and Q. F. Zhou, *Macromolecules,* 2006, **39**, 517-527.

25 S. Chen, L. Y. Zhang, L. C. Gao, X. F. Chen, X. H. Fan, Z. H. Shen and Q. F. Zhou, *J. Polym. Sci. Part A: Polym. Chem.,* 2009, **47**, 2408-2421.

26 S. Chen, C. K. Jie, H. L. Xie and H. L. Zhang, *J. Polym. Sci. Part A: Polym. Chem.,* 2012, **50**, 3923-3935.

27 X. C. Liang, X. F. Chen, C. Y. Li, Z. H. Shen, X. H. Fan and Q. F. Zhou, *Polymer,* 2010, **51**, 3693-3705.

28 L. Chen, Y. W. Chen, D. J. Zha and Y. Yang, *J. Polym. Sci. Part A: Polym. Chem.,* 2006, **44**, 2499-2509.

29 L. Y. Zhang, S. Chen, H. Zhao, Z. H. Shen, X. F. Chen, X. H. Fan and Q. F. Zhou, *Macromolecules,* 2010, **43**, 6024-6032.

30 Q. Yang, H. Jin, Y. D. Xu, P. Wang, X. C. Liang, Z. H. Shen, X. F. Chen, D. C. Zou, X. H. Fan and Q. F. Zhou, *Macromolecules,* 2009, **42**, 1037-1046.

31 C. Pugh and R. R. Schrock, *Macromolecules,* 1992, **25**, 6593-6604.

32 S. V. Arehart and C. Pugh, *J. Am. Chem. Soc.*, 1997, **119**, 3027-3029.

33 C. Pugh, J. Y. Bae, J. Dharia, J. J. Ge and S. Z. D. Cheng, *Macromolecules,* 1998, **31**, 5188-5200.

34 G. H. Kim, C. Pugh and S. Z. D. Cheng, *Macromolecules,* 2000, **33**, 8983-8991.

35 H. Yang, F. Zhang, B. Lin, P. Keller, X. Zhang, Y. Sun and L. Guo, *J. Mater. Chem. C,* 2013, **1**, 1482-1490.

36 Y. F. Zhu, Z. Y. Zhang, Q. K. Zhang, P. P. Hou, D. Z. Hao, Y. Y. Qiao, Z. H. Shen, X. H. Fan and Q. F. Zhou, *Macromolecules,* 2014, **47**, 2803-2810.

37 M. Warner and E. Terentjev, *Liquid Crystal Elastomers*, Oxford University Press, Oxford, UK, 2003.

38 T. Ikeda, J. Mamiya and Y. Yu, *Angew. Chem. Int. Ed.,* 2007, **46**, 506-528.

39 C. Ohm, M. Brehmer and R. Zentel, *Adv. Mater.,* 2010, **22**, 3366-3387.
40 D. L. Thomsen III, P. Keller, J. Naciri, R. Pink, H. Jeon, D. Shenoy and B. R. Ratna, *Macromolecules,* 2001, **34**, 5868-5875.
41 Z. L. Wu, A. Buguin, H. Yang, J. M. Taulemesse, N. Le Moigne, A. Bergeret, X. Wang, and P. Keller, *Adv. Funct. Mater.,* 2013, **23**, 3070-3076.
42 E. Anglaret, M. Brunet, B. Desbat, P. Keller and T. Buffeteau, *Macromolecules*, 2005, **38**, 4799-4810.
43 B. Neises and W. Steglich, *Angew. Chem.*, 1978, **90**, 556-557.
44 K. Ishihara and N. Nakajima, *J. Mol. Cat. B: Enzym.*, 2003, **23**, 411-417.
45 O. Mitsunobu, *Synthesis,* 1981, 1-28.
46 http://www.sigmaaldrich.com/content/dam/sigma-aldrich/docs/Aldrich/General_Information/thermal_initiators.pdf
47 C. Ye, H. L. Zhang, Y. Huang, E. Q. Chen, Y. L. Lu, D. Y. Shen, X. H. Wan, Z. H. Shen, S. Z. D. Cheng and Q. F. Zhou, *Macromolecules*, 2004, **37**, 7188-7196.
48 C. Y. Li, K. K. Tenneti, D. Zhang, H. L. Zhang, X. H. Wan, E. Q. Chen, Q. F. Zhou, A. O. Carlos, S. Igos and B. S. Hsiao, *Macromolecules*, 2004, **37**, 2854-2860.
49 De Gennes and P. G.; Prost, J. *The Physics of Liquid Crystals*, 2nd ed., Clarendon: Oxford, 1993.
50 D. M. Walba, H. Yang, R. K. Shoemaker, P. Keller, D. A. Coleman, C. D. Jones, M. Nakata and N. A. Clark, *Chem. Mater.,* 2006, **18**, 4576-4584.
51 H. Yang, L. Wang, R. Shao, N. A. Clark, J. Ortega, J. Etxebarria, P. A. Albouy, D. M. Walba and P. Keller, *J. Mater. Chem.,* 2009, **19**, 7208-7215.
52 H. Yang, M. Liu, Y. Yao, P. Tao, B. Lin, P. Keller, X. Zhang, Y. Sun and L. Guo, *Macromolecules,* 2013, **46**, 3406-3416.
53 H. Yang, Y. J. Lv, B. P. Lin, X. Q. Zhang, Y. Sun and L. X. Guo, *J. Polym. Sci. Part A: Polym. Chem.,* 2014, **52**, 1086-1098.
54 P. G. De Gennes, *Phys. Lett. A,* 1969, **28**, 725-726.
55 W. Wu, L.Yao, T.Yang, R. Yin, F. Li and Y.Yu, *J. Am. Chem. Soc.,* 2011, **133**, 15810-15813.
56 H. Yang, J. J. Liu, Z. F. Wang, L. X. Guo, P. Keller, B. P. Lin, Y. Sun and X. Q. Zhang, *Chem. Commun.,* 2015, **51**, 12126-12129.
57 W. Lehmann, H. Skupin, C. Tolksdorf, E. Gebhard, R. Zentel, P. Kruger, M. Losche and F. Kremer, *Nature,* 2001, **410**, 447-450.
58 A. Kaiser, M. Winkler, S. Krause, H. Finkelmann and A. M. Schmidt, *J. Mater. Chem.,* 2009, **19**, 538-543.
59 M. Yamada, M. Kondo, J. I. Mamiya, Y. L.Yu, M. Kinoshita, C. J. Barrett and T. Ikeda, *Angew. Chem. Int. Ed.,* 2008, **47**, 4986-4988.
60 H. Yang, A. Buguin, J. M. Taulemesse, K. Kaneko, S. Mery, A. Bergeret and P. Keller, *J. Am. Chem. Soc.,* 2009, **131**, 15000-15004.
61 C. L. Van Oosten, C. W. M. Bastiaansen and D. J. Broer, *Nat. Mater.,* 2009, **8**, 677-682.
62 K. D. Harris, C. W. M. Bastiaansen, J. Lub and D. J. Broer, *Nano Lett.,* 2005, **5**, 1857-1860.
63 C. Ohm, C. Serra and R. Zentel, *Adv. Mater.,* 2009, **21**, 4859-4862.
64 H. Yang, G.Ye, X. Wang and P. Keller, *Soft Matter,* 2011, **7**, 815-823.
65 C. Ohm, N. Kapernaum, D. Nonnenmacher, F. Giesselmann, C. Serra and R. Zentel, *J. Am. Chem. Soc*., 2011, **133**, 5305-5311.
66 E.-K. Fleischmann, H.-L. Liang, N. Kapernaum, F. Giesselmann, J. Lagerwall and R. Zentel, *Nat. Commun.,* 2012, **3**, 1178.
67 T. Ikeda, M. Nakano, Y. L.Yu, O. Kanazawa and Tsutsumi, A. *Adv. Mater.,* 2003, **15**, 201-205.

Table of Contents Graphic

Poly(Vinyl Benzoate)-Backbone Mesogen-Jacketed Liquid Crystalline Polymers

Hong Yang,*[a] You-Jing Lv,[a] Ming Xu,[a] Jun Wang,[b] Bao-Ping Lin,[a] Ling-Xiang Guo,[a] and Er-Qiang Chen*[b]

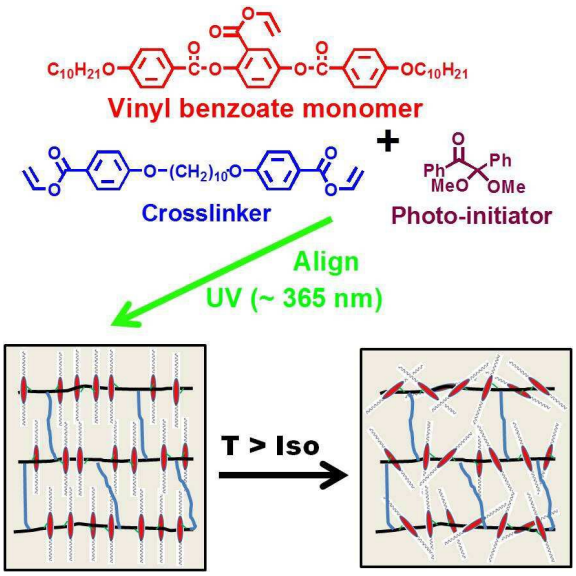

This work describes a new system, poly(vinyl benzoate)-backbone MJLCPs which are efficiently synthesized by bulk photo-polymerization method. Furthermore, by UV-illumination on an oriented mixture of vinylbenzoate monomers and crosslinkers, homogeneous- or homeotropic-aligned cross-linked MJLCP (xMJLCP) films are for the first time successfully prepared.